Contribution from the Department of Chemistry,
Indiana University, Bloomington, Indiana 47405

Hydroxycarbene Complexes from Paramagnetic Acylmetals. Electrochemistry of Benzoylchromium(0) and -tungsten(0) Carbonyls

R. J. KLINGLER, J. C. HUFFMAN, and J. K. KOCHI*

Received May 6, 1980

The group 6 acylmetal(0) anions $RCOCr(CO)_5^-$ and $RCOW(CO)_5^-$ yield paramagnetic acylchromium(I) and -tungsten(I) species upon anodic oxidation. Ion-pairing effects with various cations are shown by the shifts of the cyclic voltammetric peak potentials and in the carbonyl IR frequencies of $PhCOCr(CO)_5^-$. The benzoylchromium(I) radical is sufficiently persistent at low temperatures to observe its well-resolved ESR spectrum, but it is readily converted to the hydroxycarbene complex $Ph(HO)C{=}Cr(CO)_5$ by hydrogen atom transfer. The X-ray crystallographic determination of $Ph(HO)C{=}Cr(CO)_5$ elucidates the structural consequences of strong hydrogen bonding to the hydroxy group in cyclic voltammetric studies of the carbene complex.

Introduction

Transition-metal acyl derivatives are important intermediates in a variety of catalytic processes, especially with carbon monoxide,[1] and they are also useful as synthetic reagents.[2] However, virtually all of the known chemistry of this important class of organometallic complexes is based on stable diamagnetic compounds. The increasing awareness of the importance of organometallic radicals in many transformations such as oxidative addition,[3] substitution,[4] and hydrogenation[5] has encouraged us to reexamine the chemistry of acylmetals in this light.

Electrochemical techniques offer a potentially general method of generating reactive paramagnetic intermediates which otherwise would be too unstable to isolate by standard chemical means. In this study, our principal goal is to establish the feasibility of producing transient acylmetal radicals and to employ electrochemical techniques as well as electron spin resonance spectroscopy to characterize the intermediates. The identification of the mechanistic pathways for reaction and the isolation of the products from these paramagnetic acylmetals are also important objectives.

Results and Discussion

The electrochemistry of the anionic group 6 acylmetal(0) carbonyls of the general class

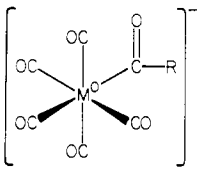

where M = tungsten or chromium and R = alkyl, allyl, and substituted phenyl, was examined at 25 °C. The salts were prepared and isolated as the tetraethylammonium derivatives to allow solubility in acetonitrile, the electrochemical medium.

Cyclic Voltammetry of Acylchromium(0) and -tungsten(0) Carbonyls. The single-sweep cyclic voltammogram (CV) of benzoylpentacarbonylchromium(0) at a platinum microelectrode is depicted in Figure 1. The voltammogram taken at −78 °C and a sweep rate of 10 V s^{-1} shows indications of being quasi-reversible (eq 1), since the current ratio of the cathodic

$$PhCOCr^0(CO)_5^- \rightleftharpoons PhCOCr^I(CO)_5 + e^- \qquad (1)$$

and anodic peaks $i_p(c)/i_p(a)$ approached unity at a peak voltage separation $E_p(c) - E_p(a)$ of 150 mV. [We were unable to manipulate the temperature sufficiently to make a significant improvement in this CV.]

Table I. Cyclic Voltammetric Parameters for Acylchromium(0) and -tungsten(0) Carbonyls[a]

acylmetal anion[b] $RCOM(CO)_5^-$	$E_p(1)$,[c] V	$E_p(2)$,[c] V	$i_p(c)/i_p(a)$[d]
$CH_3COW(CO)_5^-$	0.30	0.95	*e*
$C_6H_5COW(CO)_5^-$	0.15	1.03	*e*
$CH_2{=}CHCH_2COW(CO)_5^-$	0.07	0.64	*e*
$CH_3COCr(CO)_5^-$	0.50	1.01	*e*
$C_6H_5COCr(CO)_5^-$	0.40	0.92	0.67[f]
p-$CH_3C_6H_4COCr(CO)_5^-$	0.18	0.89	*e*
p-$FC_6H_4COCr(CO)_5^-$	0.55	1.08	*e*
p-$CH_3OC_6H_4COCr(CO)_5^-$	0.53	1.05	*e*
$Me_3SiCH_2COCr(CO)_5^-$	0.24	0.87	*e*

[a] In 0.1 M tetraethylammonium perchlorate solutions of acetonitrile at 25 °C. [b] 10^{-3} M as tetraethylammonium salt. [c] Voltage relative to saturated NaCl-SCE. [d] Ratio of cathodic and anodic peak currents at 0.1 V s^{-1}. [e] Cathodic wave not observed. [f] At −25 °C, cathodic and anodic peak potential separation of 150 mV.

Chronoamperometric studies (described in detail in the Experimental Section) indicate a lifetime for the benzoylchromium(I) radical $PhCOCr^I(CO)_5$ to be approximately 20 ms. The lifetime of the acetyl analogue $CH_3COCr^I(CO)_5$ must be even shorter, since the initial anodic scan of the cyclic voltammogram showed no cathodic wave on the reverse scan even at sweep rates as high as 10 V s^{-1}. The cyclic voltammograms of the other acylchromium complexes listed in Table I exhibit similar anodic peaks, the potentials $E_p(1)$ of which vary with the nature of the acyl ligand. Similarly, the analogous tungsten carbonyls $RCOW(CO)_5^-$ are irreversibly oxidized in the region between 0.1 and 0.5 V vs. SCE. Furthermore, all the derivatives also showed a second irreversible anodic CV wave at approximately 1 V. Since $PhCOCr(CO)_5^-$ was the best behaved of the acylmetal derivatives, we focus our attention now on the electrochemistry and the structural identification of the benzoylchromium(I) species.

ESR Detection of the Paramagnetic Benzoylchromium(I) Species. The benzoylchromium(I) species produced by the anodic oxidation of $PhCOCr(CO)_5^-$ is too transient to observe its ESR spectrum by conventional means. Instead, a flow cell utilizing a microporous silver electrode[6] was inserted directly

(1) (a) Pruett, R. L. *Adv. Organomet. Chem.* **1979**, *17*, 1. (b) Forster, D. *Ibid.* **1979**, *17*, 255. (c) Kochi, J. K. "Organometallic Mechanisms and Catalysis"; Academic Press: New York, 1978; Chapter 14.
(2) (a) King, R. B. *Acc. Chem. Res.* **1970**, *3*, 417. (b) King, R. B.; Bisnette, M. B. *J. Organomet. Chem.* **1964**, *2*, 15. (c) Collman, J. P. *Acc. Chem. Res.* **1975**, *8*, 342.
(3) (a) Bradley, J. S.; Connor, D. E.; Dolphin, D.; Labinger, J. A.; Osborn, J. A. *J. Am. Chem. Soc.* **1972**, *94*, 4043. (b) Labinger, J. A.; Kramer, A. V.; Osborn, J. A. *Ibid.* **1973**, *95*, 7908. (c) Tsou, T. T.; Kochi, J. K. *Ibid.* **1979**, *101*, 6319.
(4) Byers, B. H.; Brown, T. L. *J. Am. Chem. Soc.* **1977**, *99*, 2527. (b) Wegman, R. W.; Brown, T. L. *Ibid.* **1980**, *102*, 2494.
(5) (a) Feder, H. M.; Halpern, J. *J. Am. Chem. Soc.* **1975**, *97*, 7186. (b) Sweany, R. L.; Halpern, J. *Ibid.* **1977**, *99*, 8335. (c) Klingler, R. J.; Mochida, K.; Kochi, J. K. *Ibid.* **1979**, *101*, 6626.
(6) Kenkel, J. V.; Bard, A. *J. Electroanal. Chem. Interfacial Electrochem.* **1974**, *54*, 47.

0020-1669/81/1320-0034$01.00/0

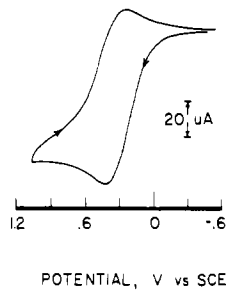

Figure 1. Initial scan cyclic voltammogram of 1.2×10^{-3} M $[Et_4N][PhCOCr(CO)_5]$ in acetonitrile at −78 °C containing 0.10 M tetra-*n*-butylammonium perchlorate at a platinum microelectrode with a scan rate of 10 V s^{-1}.

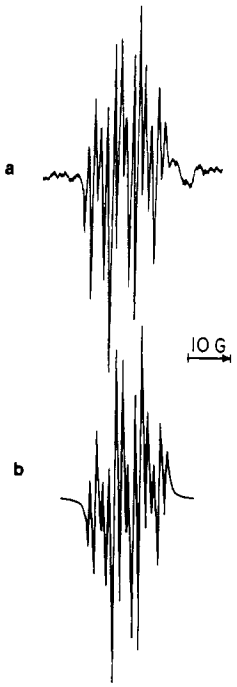

Figure 2. (a) ESR spectrum obtained at −40 °C during the anodic oxidation of 5×10^{-3} M $[Et_4N][PhCOCr(CO)_5]$ in 0.1 M TEAP in acetonitrile at 0.15 V vs. SCE. (b) Computer simulated spectrum using the ESR parameters listed in Table II and line widths of 0.70 G.

into the ESR cavity, and a 10^{-3} M solution of $[Et_4N][PhCOCr(CO)_5]$ in acetonitrile was continuously electrolyzed at 0.15 V vs. SCE at −40 °C. The resultant ESR spectrum shown in Figure 2a disappears immediately when the current through the cell is interrupted. The hyperfine splittings in the spectrum can be successfully assigned to a pair of 1:3:1 triplets and a doublet for the five aromatic protons of the benzoyl group, as indicated by a comparison with the computer-simulated spectrum in Figure 2b. The hyperfine splitting due to ^{53}Cr in 9.5% natural abundance with $I = {}^3/_2$ was not observed. [Anodic oxidation of the tungsten analogue $PhCOW(CO)_5^-$ (in which the metal splitting for ^{183}W in 14.3% natural abundance with $I = {}^1/_2$ should be more readily discerned) unfortunately did not yield any observable ESR signal consistent with the lack of reversibility of the cyclic voltammetric experiments at this temperature.] The magnitudes of the aromatic proton hyperfine splittings for $PhCOCr^I(CO)_5$ are compared in Table II with those for various related organic radical fragments, viz., the benzaldehyde radical anion,[7] as

Table II. Aromatic Proton Hyperfine Splittings (G) in Benzoylchromium(I) and Related Organic Radicals[a]

	$PhCOCr^I(CO)_5$	$PhCHO^{-\cdot}$	$PhCHOH$	$PhCO$	$Ph\cdot$
ortho	4.63 (8)[b]	4.7	4.6	<0.1	17.43
meta	1.58 (8)	1.3	1.6	1.16	6.25
para	6.00 (8)	6.5	5.9	<0.3	2.04

[a] From ref 7-9 (see text). [b] Number in parentheses refers to the estimated error in the least significant digit.

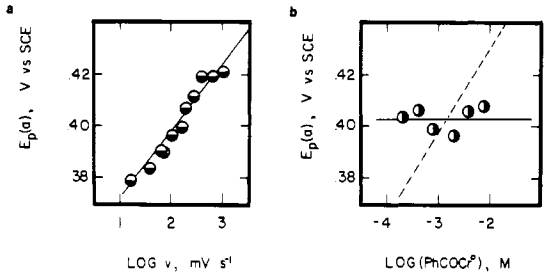

Figure 3. Dependence of the cyclic voltammetric peak potential on (a) the scan rate and (b) the concentration of $[PhCOCr(CO)_5^-]$ in 0.1 M TEAP in acetonitrile solution at 25 °C. In part a the concentration of $[PhCOCr(CO)_5^-]$ is 4×10^{-3} M, and in part b the sweep rate v is 100 mV s^{-1}. The voltage is relative to saturated NaCl-SCE.

well as α-hydroxybenzyl,[8] benzoyl,[9] and phenyl[10] radicals, as illustrated together with their isotropic $\langle g \rangle$ values:

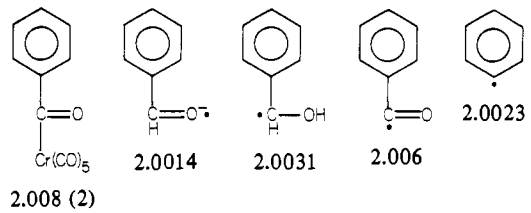

There are two features about the ESR parameters above and those in Table II which are especially noteworthy. First, the absolute magnitudes of the proton hyperfine splittings (hfs) in the benzoylchromium(I) radical are strikingly similar to those previously observed in the benzaldehyde radical anion and α-hydroxybenzyl radical. Moreover, these hfs constants are readily distinguished from those in either the benzoyl radical or the phenyl radical. Second, the relatively large magnitude of the isotropic g value of the benzoylchromium(I) radical compared to its organic analogues reflects in part the large spin–orbit coupling constant of chromium (e.g., 230 cm^{-1} for Cr^{2+}).[11]

Chemical Reactivity of Benzoylchromium(I) Radical. The electrochemical oxidation of the anionic benzoylchromium(0) carbonyl leads to the highly labile paramagnetic intermediate $PhCOCr^I(CO)_5$ which can be observed directly by ESR spectroscopy at low temperatures. We now wish to delineate the chemistry associated with this interesting organometallic radical, particularly with regard to the kinetics, the products, and the ion-pairing effects.

(1) Kinetics. Electrochemical theory is well developed for determining the various rate processes associated with labile

(7) (a) Steinberger, N.; Fraenkel, G. K. *J. Chem. Phys.* **1964**, *40*, 723. (b) Kaminski, W.; Möbius, K. *J. Magn. Reson.* **1971**, *5*, 182. (c) Hirota, N. In "Radical Ions"; Kaiser, E. T., Kevan, L., Eds.; Wiley-Interscience: New York, 1968; p 35 ff.

(8) (a) Atkins, P. W.; Frimston, J. M.; Frith, P. G.; Gurd, R. C.; McLauchlan, K. A. *J. Chem. Soc., Faraday Trans. 2* **1973**, 1542. (b) Wilson, R. *J. Chem. Soc. B* **1968**, 84. (c) Livingston, R.; Zeldes, H. *J. Chem. Phys.* **1966**, *44*, 1245.

(9) (a) Paul, H.; Fischer, H. *Helv. Chim. Acta.* **1973**, *56*, 1575. (b) Krusic, P. J.; Rettig, T. A. *J. Am. Chem. Soc.* **1970**, *92*, 722.

(10) (a) Zemel, H.; Fessenden, R. W. *J. Phys. Chem.* **1975**, *79*, 1419. (b) Kasai, P. H.; Clark, P. A.; Whipple, E. B. *J. Am. Chem. Soc.* **1970**, *92*, 2640. (c) Kasai, P. H.; Hedaya, E.; Whipple, E. B. *Ibid.* **1969**, *91*, 4364.

(11) Wertz, J. E.; Bolton, J. R. "Electron Spin Resonance"; McGraw-Hill: New York, 1972. (b) Also compare some related d^5 organoiron(III) complexes which exhibit significantly larger g values: Klingler, R. J.; Kochi, J. K. *J. Organomet. Chem.*, in press.

Table III. Cation Effects on the Anodic Peak Potential and the IR Carbonyl Frequencies of $PhCOCr(CO)_5^-$ [a]

cation M^{n+}	E_p, [b] V	carbonyl frequency, cm^{-1}		
		ν_1	ν_2	ν_3
Et_4N^+	0.40_0	2030	1895	1865
Na^+	0.41_3	2030	1898	1870
Li^+	0.42_0	2030	1910	1875
Ni^{2+}	0.42_8	2040	1935	1898
Ba^{2+}	0.45_0	2030	1900	1880
Zn^{2+}	0.46_8	2040	1940	1890
Mn^{2+}	0.48_3	2030	1908	1900
Mg^{2+}	0.50_0	2040	1913	1900

[a] In acetonitrile solution at 20 °C in the presence of 0.20 M $M(ClO_4)_n$ and 2×10^{-3} M $[Et_4N][PhCOCr(CO)_5]$. [b] Measured at a scan rate of 100 mV s^{-1}; voltage relative to saturated NaCl-SCE.

electrogenerated species.[12] The cyclic voltammetric peak potential E_p is the most sensitive and convenient probe for our purposes. Thus the dependence of E_p on the scan rate v is depicted in Figure 3a for the anodic oxidation of $PhCOCr(CO)_5^-$. The observed slope of 30 mV/decade is consistent with the first-order decay of $PhCOCr^I(CO)_5$. The latter is also supported by the absence of any trend in the peak potential with the concentration of $PhCOCr(CO)_5^-$ in Figure 3b, as required for a first-order decay process. If the benzoylchromium(I) radical were disappearing by a second-order reaction, the slope in Figure 3b would be 30 mV/decade,[12,13] as indicated by the dashed line. Electrochemical kinetics thus provides the clear evidence that the transitory $PhCOCr^I(CO)_5$ disappears by a first-order process to afford the products described in the next section.

(2) Products. Bulk electrolysis at 0 °C of an acetonitrile solution of $[Et_4N][PhCOCr(CO)_5]$ with a platinum gauze electrode at +0.40 V vs. SCE required 0.93 ± 0.05 electrons/Cr. The initially pale yellow solution progressively darkened to a deep red solution (λ_{max} 435 nm) at the end of the electrolysis. The red neutral product was separated from the acetonitrile solution by extraction with pentane at 0 °C. Concentration of the pentane extract in vacuo, followed by cooling to −78 °C, afforded dark red crystals of the hydroxycarbene complex $(OC)_5Cr{=}C(OH)C_6H_5$ which was identified by comparison of its IR and ^1H NMR spectra with those of an authentic sample.[14] The hydroxycarbene complex was formed in 70% yield, judging from the intensity of the carbonyl band at 1945 cm^{-1} in the solution after electrolysis. The acetonitrile complex of chromium(0) tetracarbonyl $Cr(CO)_4(NCCH_3)_2$ was isolated as a minor product (see Experimental Section). It is formed in 10% yield, as determined by cyclic voltammetry of the crude reaction mixture after bulk electrolysis by using the anodic wave at E_p = 0.53 V of an authentic sample[15] for calibration. Gas chromatographic analysis of the electrolyzed solution indicated the presence of benzene as a minor product (8%). Neither benzaldehyde nor benzophenone was observed, although the addition of authentic samples showed that a 1% yield of these compounds would have been detected. Finally, the observation of methane and ethylene is elaborated in the following section.

(3) Ion-Pairing Effects. The Lewis acidity of the countercation M^+ has an important effect on the ion pairing of anions in solution.[16,17] As applied to the benzoylchromium(0) anion examined in this study, a pertinent ion-pair equilibrium may be represented as eq 2. We have observed the effects

$$(OC)_5CrC(=O)Ph^-M^+ \rightleftharpoons (OC)_5Cr{=}C(OM)Ph \quad (2)$$

of such an ion pairing in two ways: first, on the cyclic voltammetric peak potentials as well as the carbonyl frequencies in the IR spectrum of $[M][PhCOCr(CO)_5]$ and, second, on the products derived from the benzoylchromium(I) radical.

The effect of cations on the CV peak potentials of $PhCOCr(CO)_5^-$ was examined in acetonitrile solutions by adding various perchlorates $M(ClO_4)_n$ as the supporting electrolyte. As shown in Table III, there is a progressive increase in the anodic peak potential starting from $M = Et_4N^+$, up to the univalent cations Na^+ and Li^+, and through the divalent cations Ni^{2+}, Ba^{2+}, Zn^{2+}, and Mg^{2+}. Within each class, the highest E_p is generally associated with the smallest cation, reflecting in part the importance of charge density. In other words, the general trend in the anodic peak potentials accords with expected order for an electrostatic interaction with a hard oxygen-centered base.[18] Such an effect is manifested in the amount of electron density available for π back-donation in the carbonyl ligands, as measured by the carbonyl frequencies in the IR spectra in Table III. The graphic representation in Figure 4 of the low-energy IR band ν_3 as a function of E_p clearly bears out this mechanistic formulation.[21]

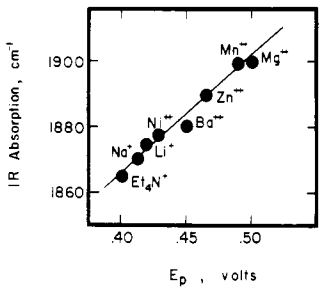

Figure 4. Ion-pairing effects in the cyclic voltammetry and the IR carbonyl absorption bands ν_3 of anionic benzoylpentacarbonylchromium(0) in the presence of 0.2 M $M(ClO_4)_n$ in acetonitrile solutions at 25 °C.

Table IV. Effect of Cations on the Yield of Hydroxycarbene from Benzoylchromium(I) Radicals[a]

$M(ClO_4)_n$ M^+	% $Ph(HO)C{=}Cr(CO)_5$	% $CH_2{=}CH_2$
Na^+	0	0
Et_4N^+	70	5
$EtPh_3P^+$	66	9
Et_3PhP^+	68	10

[a] In acetonitrile solutions of 3×10^{-2} M $PhCOCr(CO)_5^-$ containing 0.2 M $M(ClO_4)_n$ after bulk electrolysis at 0 °C and 0.40 V vs. NaCl-SCE.

(12) (a) Pletcher, D. *Chem. Soc. Rev.* **1975**, *75*, 1190. (b) Streitwieser, A. In "Physical Methods of Chemistry"; Weissberger, A., Rossiter, B. W., Eds.; Wiley-Interscience: New York, 1971; Part IIA.
(13) (a) Saveant, J. M.; Vianello, E. *C. R. Hebd. Seances Acad. Sci.* **1963**, *256*, 2597. (b) Nicholson, R. S.; Shain, I. *Anal. Chem.* **1964**, *36*, 706.
(14) (a) Fischer, E. O.; Kreis, G.; Kreissl, F. R. *J. Organomet. Chem.* **1973**, *56*, C37. (b) Weiss, K.; Fischer, E. O. *Chem. Ber.* **1976**, *109*, 1120.
(15) Strohmeier, V. W.; Gerlach, K. *Chem. Ber.* **1961**, *94*,
(16) Szwarc, M. "Ions and Ion Pairs in Organic Reactions"; Wiley-Interscience: New York, 1972, 1974; Vol. 1, Vol. 2.
(17) (a) Collman, J. P.; Finke, R. G.; Cawse, J. N.; Brauman, J. I. *J. Am. Chem. Soc.* **1977**, *99*, 2515. (b) Darensbourg, M.; Barros, H.; Borman, C. *Ibid.* **1977**, *99*, 1647. (c) Darensbourg, M. Y.; Darensbourg, D. J.; Burns, D.; Drew, D. A. *Ibid.* **1976**, *98*, 3127. (d) Chen, K. S.; Foster, T.; Wan, J. K. S. *Can. J. Chem.* **1979**, *57*, 600.
(18) Similar ion-pair effects have been noted and studied systematically in terms of the crystal radius of the cation for the reduction of nitrobenzenes and quinones.[19] This interaction energy and related solvent dependence has been reviewed.[20]
(19) (a) Holleck, L.; Becher, D. *J. Electroanal. Chem.* **1962**, *4*, 321. (b) Peover, M. E.; Davies, J. D. *J. Electroanal. Chem.* **1963**, *6*, 46.
(20) Peover, M. E. *Electroanal. Chem.* **1967**, *2*, 1.
(21) The analysis of the IR spectra of the $XM(CO)_5$ system has been well studied.[22] The lowest energy band ν_3 of A_1 symmetry is likely to have a strong trans influence.

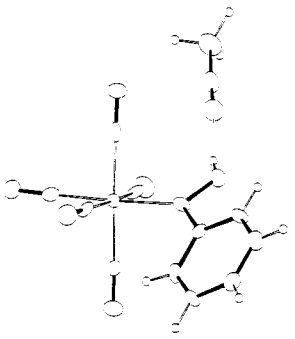

Figure 5. ORTEP drawing of the hydroxycarbene complex $[(OC)_5Cr{=}C(OH)Ph{\cdot}NCCH_3]$. All atoms are drawn at the 50% probability level.

Cations also have a striking effect on the yield of hydroxycarbene as shown in Table IV. Thus in the presence of only alkali metal cations such as Na^+, the benzoylchromium(I) radical $PhCOCr^I(CO)_5$ affords no hydroxycarbene. The observation of ethylene as a coproduct when tetraethylammonium cation is employed suggests that the source of the hydroxylic proton is derived via eq 3 and 4. [The absence of ethane

$$PhC(=O)Cr^I(CO)_5 + (CH_3CH_2)_4N^+ \rightarrow Ph(OH)C{=}Cr^0(CO)_5 + (CH_3CH_2)_3N^+CH_2CH_2\cdot \quad (3)$$

$$(CH_3CH_2)_3N^+CH_2CH_2\cdot \rightarrow CH_2{=}CH_2 + (CH_3CH_2)_3N^+\cdot, \text{ etc.} \quad (4)$$

(<0.1% by standard addition) rules out ethyl radicals as a precursor for ethylene.] The abstraction of a hydrogen atom by the benzoylchromium(I) radical in eq 3 is highly reminiscent of the well-known behavior of organic oxygen-centered radicals.[23] It also accords with the rather positive oxidation potential of the redox couple in eq 1.[24] [Note: The conversion of the radical $PhCOCr(CO)_5$ to the hydroxycarbene $Ph(HO)C{=}Cr(CO)_5$ represents a one-electron reduction, just as the electrochemical conversion of the anion $PhCOCr(CO)_5^-$ to the radical $PhCOCr(CO)_5$, as the microscopic reverse equivalent, is a one-electron oxidation.] Finally, the fragmentation to yield ethylene in eq 4 is a characteristic of β-ammonio substituents in ethyl radicals.[25] A similar process is found with the ethylphosphonium cations in Table IV, which is also consistent with the formulation in eq 3 and 4.

Structure of (Phenylhydroxycarbene)pentacarbonylchromium(0). Hydrogen Bonding Effects. The X-ray diffraction data were collected at −173 °C to reduce thermal vibrations and permit the location and refinement of all hydrogen atoms including the unique hydroxylic proton in $Ph(HO)C{=}Cr(CO)_5$. The molecular structure presented in Figure 5 shows the $Cr(CO)_5$ moiety with approximate C_{4v} symmetry. As such, it allows us to make a detailed comparison of the hydroxycarbene ligand with the amino- and alkoxycarbenoid structures containing the same $Cr(CO)_5$ unit.[26,27]

Table V. Acid Titration of $PhCOCr(CO)_5^-$ to the Phenylhydroxycarbene Complex[a]

equiv of CF_3CO_2H	i_p,[b] μA	i_p,[c] μA	Σi_p, μA
0	115	0	115
0.1	104	9	113
0.2	98	15	113
0.4	93	22	115
0.6	85	27	112
0.8	70	46	116
1.0	65	46	111

[a] Acetonitrile solution of 3×10^{-3} M $[Et_4N][PhCOCr(CO)_5]$ with 0.1 M TEAP at 25 °C. [b] Measured at 0.40 V vs. NaCl-SCE. [c] Measured at 0.50 V vs. NaCl-SCE.

Table VI. Comparative Structural Parameters of Carbene Complexes of Pentacarbonylchromium Analogues

bond length or angle	$(OC)_5Cr{=}C(OH)Ph$	$(OC)_5Cr{=}C(OCH_3)Ph$	$(OC)_5Cr{=}C(NEt_2)CH_3$
Cr=C, Å	2.05 (1)[a]	2.04 (3)[b]	2.16 (1)[c]
$=C^{O}$, Å	1.32 (1)	1.33 (2)	
C^{O}_{C}, deg	107 (1)	104 (2)	114 (1)
OC-Cr(trans), Å	1.87 (1)	1.87 (2)	1.85 (1)
OC-Cr(cis), Å	1.91 (1)	1.89 (2)	1.90 (1)

[a] This work. [b] From ref 27. [c] From ref 26.

(1) Hydrogen Bonding in (Hydroxycarbene)chromium(0). The hydrogen bonding to the acetonitrile of crystallization is clearly evident in Figure 5, in which the relevant bond distances are O–H = 0.76 Å and N–H = 1.68 Å. The strength of this interaction is also indicated by the retention of acetonitrile, despite drying the crystal in vacuo for 20 min at 0 °C followed by recrystallization from pentane. Another indication of hydrogen bonding in the hydroxyphenylcarbene complex is obtained from cyclic voltammetric studies of the protonation of the benzoylchromium(0) anion in solution by various acids, i.e., eq 5. The CV analysis of the mixture in eq 5 shows two

$$(OC)_5CrC(=O)Ph^- + HX \overset{K}{\rightleftharpoons} (OC)_5Cr{=}C(OH)Ph + X^- \quad (5)$$

anodic waves, the relative peak currents of which vary with the amount of added acid, as shown in Table V for trifluoroacetic acid. The anodic wave at $E_p = 0.40$ V corresponds to that of the benzoylchromium(0) anion, and that a 0.50 V represents the phenylhydroxycarbene complex, as described in eq 5 ($X = O_2CCF_3$). Although the latter E_p does not shift significantly during the course of acid titration,[28] it is highly sensitive to the strength of the acid. For example, $E_p = 0.50$ V for trifluoroacetic acid increases to 0.86 V when sulfuric acid is employed. Similarly, perchloric acid (used as only a 70% aqueous solution) afforded a new anodic wave at 0.80 V. However, acetic acid is too weak to protonate the anionic $PhCOCr(CO)_5^-$ to any significant degree, and no new anodic wave is observed. These results suggest that hydrogen bonding to the conjugate base X^-, similar to that in the crystal in Figure 5, is also important in acetonitrile solution (eq 6).[29]

$$(OC)_5Cr{=}C(OH)Ph + X^- \rightleftharpoons (CO)_5Cr{=}C(OH\cdots X^-)Ph \quad (6)$$

(22) (a) Wilford, J. B.; Stone, F. G. A. *Inorg. Chem.* **1965**, *4*, 389. (b) Darensbourg, M. Y.; Darensbourg, D. J. *Ibid.* **1970**, *9*, 32. (c) Huggins, D. K.; Kaesz, H. D. *J. Am. Chem. Soc.* **1964**, *86*, 2734. (d) Braterman, P. S. "Metal Carbonyl Spectra"; Academic Press: New York, 1975; p 70 ff.

(23) Kochi, J. K. In "Free Radicals"; Kochi, J. K., Ed.; Wiley: New York; Vol. II, p 665.

(24) By contrast, the oxidation potential $E^0 = +2.4$ V for the benzaldehyde anion radical makes it an excellent reducing agent, compared to $E^0 = -0.40$ V for $PhCOCr(CO)_5^-$.

(25) Kochi, J. K.; Singleton, D. M.; Andrews, L. T. *Tetrahedron* **1968**, *24*, 3503.

(26) (a) Baikie, P. E.; Fischer, E. O.; Mills, O. S. *Chem. Commun.* **1967**, 1199. (b) Connor, J. A.; Mills, O. S. *J. Chem. Soc. A* **1969**, 334. (c) Hüttner, G.; Lange, S. *Chem. Ber.* **1970**, *103*, 3149.

(27) (a) Mills, O. S.; Redhouse, A. D. *J. Chem. Soc. A* **1968**, 642. (b) Mills, O. S.; Redhouse, A. D. *Ibid.* **1969**, 1274.

(28) According to standard electrochemical theory, an acid equilibrium such as that in eq 5 will slightly affect the position of the CV peak potential. During the titration in Table V, E_p increases from 0.50 to 0.51 V. This 10-mV change is minor compared to the more than 300-mV change effected by replacing trifluoroacetic acid by sulfuric or perchloric acid.

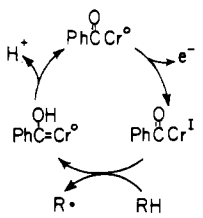

Figure 6. Catalytic interconversion of benzoylchromium species coupled to the anodic oxidation of tetraethylammonium ion.

(2) Structural Comparison of Hydroxy-, Amino- and Alkoxycarbenes as Ligands. In the structure of $Ph(HO)C{=}Cr(CO)_5$, the chromium, oxygen, and carbon atoms bonded to the carbenoid carbon are all coplanar within the experimental error, and the carbene ligand assumes a staggered configuration relative to the four cis carbonyl ligands. Indeed the same basic molecular structure pertains throughout the related series of carbene–tetracarbonylchromium(0) complexes. In Table VI, the trigonal angles about the carbenoid carbon (i.e., O–C–C) are quite similar (106 ± 1°) in the hydroxy- and methoxycarbene complexes but significantly smaller than that (114°) in the amino analogue. This difference is coupled with the slightly longer Cr=C bond distance. However, the trans influence on the chromium–carbonyl bond distance appears to be minimal.

Summary and Conclusions

Electrochemical techniques can be effectively used to examine the behavior of organometallic ions in solution. Thus, the group 6 anionic acyl complexes $Cr(CO)_5COR^-$ and $W(CO)_5COR^-$ are readily oxidized in a one-electron process at relatively low electrode potentials. Ion-pairing effects are manifested in the variation of the cyclic voltammetric peak potentials with cation structures. The latter correlates with the more conventional measurements of the changes in the carbonyl frequencies in the IR spectrum of $PhCOCr(CO)_5^-$ in the presence of various cations.

The anodic oxidations of acylchromium(0) and acyltungsten(0) anions afford paramagnetic chromium(I) and tungsten(I) species which are transient on the electrochemical time scale of 1 ms. At low temperatures, the benzoylchromium(I) radical $PhCOCr(CO)_5$ can be observed, both by cyclic voltammetry and by ESR spectroscopy. The magnitude of the proton hyperfine splittings and the isotropic g value of $PhCOCr(CO)_5$ suggest that the odd electron density is highly ligand centered. Consistent with this structural formulation, the reactive benzoylchromium(I) radical attacks the tetraethylammonium countercation by a kinetically first-order process to afford the phenylhydroxycarbene complex $Ph(HO)C{=}Cr(CO)_5$ in good yields. Hydrogen atom abstraction in this manner is akin to the well-known behavior of oxygen-centered organic radicals.

Isolation of the phenylhydroxycarbene complex $Ph(HO)C{=}Cr(CO)_5$ allows the crystal structure to be determined in which the location and refinement of all hydrogen atoms indicated the presence of a strong hydrogen bond to acetonitrile. Consistent with this structural data, the cyclic voltammetric studies of $Ph(HO)C{=}Cr(CO)_5$ support the formation of hydrogen bonds as a general property of this hydroxycarbene complex.

The sequential transformation of acylchromium species which has been demonstrated in this study, viz., eq 7 (where $RH = Et_4N^+$), *formally* represents a catalytic cycle shown in Figure 6, in which the overall transformation is tantamount to the (electrochemical) oxidation of the hydrogen donor substrate, i.e., eq 8. As such, we examined the possibility of

$$PhC(=O)Cr(CO)_5^- \xrightarrow{-e} PhC(=O)Cr(CO)_5 \xrightarrow{RH} Ph(OH)C{=}Cr(CO)_5 + R\cdot \quad (7)$$

$$RH \xrightarrow{-e} R\cdot + H^+ \quad (8)$$

utilizing other donors, particularly hydroquinone, to promote the catalytic process. Unfortunately we were unable to effect the oxidation of hydroquinone (see Experimental Section), probably owing to the facile hydrogen transfer from the intimate tetraethylammonium countercation. Nonetheless, the principle is established and deserves further study. We also wish to point out that the reductive conversion of a paramagnetic acylmetal complex to a hydroxycarbene complex in Figure 6 bears directly on the propagation sequence in the Fischer–Tropsch synthesis. Indeed, hydroxycarbene complexes were among the first intermediates postulated for the Fischer–Tropsch process on the basis of kinetic and spectroscopic measurements.[30] Since their mode of formation and subsequent reactivity has not been clearly delineated,[31] the facile homolytic transformation shown in this study merits further consideration.[32]

Experimental Section

Starting Materials. The anionic acyl complexes $[Et_4N][RCOCr(CO)_5]$ and $[Et_4N][RCOW(CO)_5]$ used in this study were prepared according to Fischer's procedure, involving the addition of the appropriate lithium alkyl or aryl to $Cr(CO)_6$ and $W(CO)_6$, respectively.[33] The group 6 metal carbonyls were obtained from Pressure Chemical Co. and were used without further purification. Reagent grade acetonitrile was purified by refluxing it over a calcium hydride, treating it with potassium permanganate, and redistilling it from P_2O_5 through a 19-plate bubble-plate Oldershaw column. Tetraethylammonium perchlorate (TEAP) was obtained from G. F. Smith Chemical Co. The metal salts $Li(ClO_4)$, $Na(ClO_4)$, $Mg(ClO_4)_2$, $Mn(ClO_4)\cdot 6H_2O$, $Zn(ClO_4)_2\cdot 6H_2O$, $Ni(ClO_4)_2\cdot 6H_2O$, and $Ba(ClO_4)_2\cdot 3H_2O$ were obtained from G. F. Smith Chemical Co. and used without further purification. Triethylphenylphosphonium iodide (kindly donated by T. T. Tsou) and ethyltriphenylphosphonium iodide (from Cincinnati Milacron Co.) were used to prepare the corresponding perchlorates by metathesis with sodium perchlorate in acetone solution. The products were recrystallized twice at −20 °C from an acetone solution and dried in vacuo for 12 h at 50 °C.

Electrochemical Measurements. Electrochemistry was performed on a Princeton Applied Research Model 173 potentiostat equipped with a Model 176 current-to-voltage converter which provided a feedback compensation for ohmic drop between the working and reference electrodes. The voltage-follower amplifier (PAR Model 178) was mounted external to the main potentiostat with a minimum length of high impedance connection to the reference electrode (for low noise pickup). Cyclic voltammograms were recorded on a Houston Series 2000 X-Y recorder. The electrochemical cell was constructed according to the design of Van Duyne and Reilley.[34] The distance between the platinum working electrode and the tip of the salt bridge was 1 mm to minimize ohmic drop. Bulk coulometry was carried out in a three-compartment cell of conventional design with a platinum gauze electrode. Complete electrolysis of 0.2-mmol electroactive material generally required 5–10 min and was graphically recorded on a Leeds and Northrup Speedomax strip-chart recorder. The current–time curve was manually integrated.

Isolation of $Ph(HO)C{=}Cr(CO)_5$. A solution of 0.134 g of $[Et_4N][PhCOCr(CO)_5]$ in 8 mL of acetonitrile containing 0.10 M

(29) Similar observations have been reported in the reduction of quinones, and they have been attributed to specific effects of hydrogen bonding, in addition to simple protonation equilibria, as in eq 6.

(30) (a) Kolbel, H.; Patzschke, G.; Hammer, H. Z. *Z. Phys. Chem.* **1966**, *48*, 145. (b) Frey, H. M. *J. Am. Chem. Soc.* **1960**, *82*, 5947.

(31) Masters, D. *Adv. Organomet. Chem.* **1979**, *17*, 61.

(32) For example, one aspect of the proposed growth sequence involves the reduction of an acylmetal with hydrogen to an alkylmetal and water. The reduction of acylmetals to hydroxycarbene complexes by hydrogen atom transfer, as described here, is a viable alternative to hydrido acylmetal species as intermediates.

(33) (a) Fischer, E. O.; Maasböl, A. *Chem. Ber.* **1967**, *100*, 2445. (b) Fischer, E. O.; Maasböl, A. *Angew. Chem., Int. Ed. Engl.* **1964**, *3*, 580.

(34) Van Duyne, R. P.; Reilley, C. N. *Anal. Chem.* **1972**, *44*, 142.

tetraethylammonium perchlorate was electrolyzed at 0 °C and 0.40 V vs. NaCl-SCE. The electrolysis was terminated after the current had decayed to 90% of its initial value. [Note: The applied voltage of 0.40 V is sufficiently positive to lie in the foot of the anodic wave of $Cr(CO)_4(NCCH_3)_2$ which is one of the side products. Thus the current could not be allowed to decay completely to zero. However, no difficulty was encountered in determining the point at which to stop the electrolysis since the initial rapid decay is followed by a much slower process.] The measured area of the current–time plot (28.8 A s) corresponded to 0.95 ± 0.05 electrons/Cr. Upon electrolysis the initially pale yellow solution turned deep red, and extraction with 20-mL portions of pentane at 0 °C was continued until the extracts were colorless. Concentration of the combined pentane extracts in vacuo, followed by cooling to −78 °C, yielded 47 mg (50%) of a red solid. ^1H NMR in C_6D_6: δ 7.78 (Ph), 11.0 (OH), 1.94 (CH_3CN). An authentic sample of $Ph(HO)C{=}Cr(CO)_5$ was prepared according to the published procedure[14] for spectral comparisons. The crude yield (70%) of $Ph(HO)C{=}Cr(CO)_5$ was ascertained from the intensity of the carbonyl bands at 1945 cm^{-1} in the IR spectrum relative to that of a standard solution of authentic material.

Identification of the Minor Products in the Electrolysis of $[Et_4N][PhCOCr(CO)_5]$. An acetonitrile solution of $[Et_4N][PhCOCr(CO)_5]$ was electrolyzed as described above. Analysis of the gaseous products over the solution by gas chromatography on a column of Porapak Q at 50 °C indicated the presence of ethylene (5%) and methane (1%). However, less than 0.01% ethane was detected by using the internal standard method. Similarly, the solvent was analyzed by gas chromatography on a 15-ft Apiezon L column at 80 °C and found to contain benzene (8%) by using a cyclohexane internal standard. The yield of benzophenone and benzaldehyde was established to be less than 1% by the method of standard addition. After removal of the hydroxycarbene complex by extraction with pentane as described above, the acetonitrile was separated in vacuo. The resultant solid was washed with water to remove the supporting electrolyte and recrystallized from methylene chloride. Its IR and ^1H NMR spectra as well as the oxidation potential corresponded to that of $Cr(CO)_4(CH_3CN)_2$ prepared by photolysis of $Cr(CO)_6$ in acetonitrile according to published procedure.[15]

Effect of Cations on the CV of $PhCOCr(CO)_5^-$. Acetonitrile solutions of 5×10^{-3} M $[Et_4N][PhCOCr(CO)_5]$ and 0.20 M metal perchlorates listed in Table III were analyzed by cyclic voltammetry at 100 mV s^{-1} and 20 °C. The infrared spectra of the solutions were examined at ambient temperatures.

Protonation of $PhCOCr(CO)_5^-$. An acetonitrile solution of 5×10^{-3} M $[Et_4N][PhCOCr(CO)_5]$ was treated in the CV cell, with incremental amounts of the appropriate acid. The initially pale yellow solution darkened perceptibly with each addition—finally acquiring the characteristic red color of the carbene complex $Ph(HO)C{=}Cr(CO)_5$. At the same time, the anodic peak current i_p due to the oxidation of $PhCOCr(CO)_5^-$ decreased in proportion to the growth of the new anodic wave at higher electrode potentials (see Table V).

Anodic Oxidation of $PhCOCr(CO)_5^-$ in the Presence of Hydroquinone. A solution of 0.14 mmol of $[Et_4N][PhCOCr(CO)_5]$ and 0.22 mmol of hydroquinone in 8 mL of acetonitrile was oxidized at 0.40 V vs. NaCl-SCE. Within experimental error, the hydroquinone was unaffected by the oxidation of the benzoylchromium(0) anion, as determined by the undiminished intensity of the OH stretching band at 3400 cm^{-1} in the IR spectrum. Moreover, no absorption for *p*-benzoquinone at 1665 cm^{-1} was observed.

X-ray Structure Analysis. A sample of $Ph(HO)C{=}Cr(CO)_5$, dissolved in pentane at 0 °C and slowly cooled to −60 °C over a 15-h period, grew as stacked prisms or polydentate needles. A dark red crystal measuring 0.12 × 0.12 × 0.09 mm was cleaved from one such cluster and mounted in a CO_2 atmosphere and transferred to the goniostat maintained at −173 °C [$CrC_{12}O_6H_6{\cdot}C_2H_3N$: M_r = 338.22; space group $P2_1/c$; at 173 °C, a = 10.778 (5) Å, b = 11.071 (6) Å, c = 13.321 (6) Å, β = 110.10 (1)°; Z = 4, V = 1492.7 Å^3; D_c = 1.505 g cm^{-3}; linear absorption coefficient 7.721 cm^{-1}].

The diffractometer utilized for data collection was designed and constructed locally. A Picker four-circle goniostat equipped with a Furnas Monochromator (HOG crystal) and Picker X-ray generator is interfaced to a T1980 minicomputer, with Slo-Syn stepping motors to drive the angles. Centering is accomplished by using automated top/bottom–left/right slit assemblies. The minicomputer is interfaced by low-speed data lines to a CYBER172-CDC6600 multimainframe system where all computations are performed.

Table VII. Fractional Atomic Coordinates[a]

atom	10^4x	10^4y	10^4z	$10B_{iso}$, Å^2
Cr(1)	3730 (1)	3723 (1)	1558 (1)	12
C(2)	3697 (7)	2258 (8)	2315 (7)	15
O(3)	3699 (6)	1357 (6)	2711 (5)	22
C(4)	3616 (8)	2781 (8)	331 (7)	18
O(5)	3667 (6)	2224 (5)	−374 (5)	23
C(6)	4027 (8)	4668 (8)	2817 (7)	17
O(7)	4262 (6)	5238 (6)	3573 (5)	25
C(8)	3726 (8)	5110 (8)	723 (7)	14
O(9)	3765 (6)	5925 (5)	210 (5)	21
C(10)	5565 (8)	3587 (8)	1990 (6)	16
O(11)	6698 (6)	3484 (6)	2273 (5)	27
C(12)	1725 (8)	3849 (8)	1206 (6)	15
O(13)	915 (6)	2954 (6)	770 (5)	18
C(14)	928 (8)	4823 (8)	1427 (7)	15
C(15)	1398 (8)	6030 (8)	1592 (7)	17
C(16)	641 (8)	6930 (8)	1785 (6)	15
C(17)	−568 (9)	6667 (8)	1883 (7)	20
C(18)	−1044 (9)	5502 (8)	1756 (7)	19
C(19)	−307 (8)	4600 (8)	1519 (7)	15
N(20)	1611 (8)	710 (8)	277 (7)	31
C(21)	1912 (8)	−209 (9)	77 (7)	22
C(22)	2252 (13)	−1421 (11)	−173 (11)	29
atom	10^3x	10^3y	10^3z	$10B_{iso}$, Å^2
H(1)	121 (8)	237 (8)	65 (7)	8 (21)
H(2)	226 (7)	615 (6)	158 (5)	1 (14)
H(3)	97 (8)	778 (8)	190 (7)	24 (19)
H(4)	−93 (7)	724 (7)	202 (5)	0 (15)
H(5)	−188 (7)	531 (6)	180 (5)	5 (14)
H(6)	−69 (8)	379 (8)	143 (6)	19 (18)
H(7)	173 (17)	−212 (16)	3 (13)	113 (53)
H(8)	214 (10)	−146 (10)	−74 (9)	39 (31)
H(9)	323 (10)	−146 (8)	18 (7)	39 (25)

[a] Numbers in parentheses in this and all following tables refer to the error in the least significant digit. The numbering scheme is

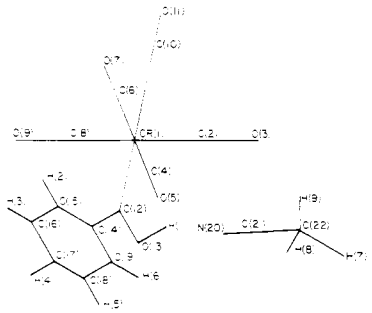

Intensity data were collected by using the $\theta/2\theta$ scan ($5° < 2\theta < 55°$); the scan rate was 2.0° min^{-1}; the single background time at the extreme of scans was 10 s. The scan width was 2.0° plus dispersions; 2634 unique reflections were collected at −173 °C, of which 1722 had $F > 2.33\sigma(F)$. Owing to the nearly equidimensional size of the crystal and the low linear absorption coefficient (7.72 cm^{-1}), no absorption correction was deemed necessary.

The structure was solved by a combination of direct methods and Patterson techniques. All computations were made with the IUMSC interactive XTEL program library which consists of a local code and selected programs adapted from those described by A. C. Larson (Los Alamos code) and J. A. Ibers (Northwestern University Library). Nonhydrogen positions located in this manner were refined isotropically; a difference Fourier synthesis, phased on the refined positions, located all hydrogen atoms. Final full-matrix refinement using anisotropic thermal parameters, and isotropic thermal parameters for hydrogen, converged rapidly. All data with $F > 2.33\sigma(F)$ (based on counting statistics) were used in the refinement. The final discrepancy factors were R = 0.085 and R_w = 0.066. The maximum δ/σ for the last cycle was 0.05, and the goodness of fit was 1.15. The fractional atomic coordinates are given in Table VII. The anisotropic thermal parameters, the observed and calculated structure factors, and the bond distances and angles are given in Tables VIII, IX, and X, respectively, in the supplementary material.

Acknowledgment. We wish to thank the M. H. Wrubel Computing Center for computational facilities and the National Science Foundation for generous financial support.

Registry No. $[Et_4N][CH_3COW(CO)_5]$, 59610-08-1; $[Et_4N][C_6H_5COW(CO)_5]$, 68866-92-2; $[Et_4N][C_3H_5COW(CO)_5]$, 75112-12-8; $[Et_4N][CH_3COCr(CO)_5]$, 75112-13-9; $[Et_4N][C_6H_5COCr(CO)_5]$, 54817-05-9; $[Et_4N][p\text{-}CH_3C_6H_4COCr(CO)_5]$, 59610-10-5; $[Et_4N][p\text{-}FC_6H_4COCr(CO)_5]$, 75112-15-1; $[Et_4N][p\text{-}CH_3OC_6H_4COCr(CO)_5]$, 75112-17-3; $[Et_4N][Me_3SiCH_2COCr(CO)_5]$, 51447-06-4; $PhCOCr^{I}(CO)_5$, 46933-82-8; $Ph(HO)C{=}Cr(CO)_5$, 50507-79-4; $CH_2{=}CH_2$, 74-85-1; $(CO)_5Cr{=}C(OH)Ph{\cdot}NCCH_3$, 75112-18-4; $Cr(CO)_4(NCCH_3)_2$, 16800-44-5; benzene, 71-43-2.

Supplementary Material Available: Complete listings of anisotropic thermal parameters (Table VIII), observed and calculated structure factors (Table IX), and bond distances and angles (Table X) (15 pages). Ordering information is given on any current masthead page.

Contribution from the Department of Chemistry and the Department of Electrical Engineering, Colorado State University, Fort Collins, Colorado 80523

Metallocene Electrochemistry. 2. Reduction–Oxidation Behavior of Nickelocene in the Room-Temperature Alkylpyridinium Chloride–Aluminum Chloride Melt System

R. J. GALE[1a] and R. JOB*[1b]

Received April 9, 1980

In neutral 1:1 molar ratio mixtures of $AlCl_3$–1-butylpyridinium chloride, at 40 °C, nickelocene undergoes a reversible 1-electron charge-transfer reaction, with $E_{1/2}$ = –0.165 V vs. Al (2:1) reference. Evidence is presented to show that both nickelocene and the nickelocenium(III) ion are unstable in chloride ion rich solvents. Spontaneous oxidation to the nickelocenium cation occurs in acidic (>1:1) melts, and a stable dication is formed reversibly at $E_{1/2}$ = +0.912 V vs. Al (2:1) reference. Electronic spectra of nickelocene species in the II, III, and IV oxidation states have been recorded in these melts. The spectrum of the dication species contains bands at 412, 438, 532 nm.

Introduction

Although the electrochemistry of the transition-metal metallocenes, particularly the effects of derivatized ferrocenes, has been investigated fairly thoroughly in both aqueous[2] and nonaqueous organic solvents,[3] only ferrocene and decamethylferrocene had been studied previously in the room-temperature $AlCl_3$–1-butylpyridinium chloride (BPC) molten salt. Chum et al.[4] were the first to study the electrochemistry of organometallic compounds in these aprotic Lewis acid solvents, and, in addition to ferrocene, they have reported the redox behaviors for two aliphatic diimine complexes of iron(II) and for six metal carbonyls, $Cr(CO)_6$, $Mo(CO)_6$, $W(CO)_6$, $Fe(CO)_6$, $Re_2(CO)_{10}$, and $Mn_2(CO)_{10}$.[5] Robinson and Osteryoung[6] observed that the ferrocene oxidation potential was independent of the melt acidity (cyclic voltammetric $E_{p/2}$ = 0.24 V vs. Al (2:1) reference), and they determined the values of the diffusion coefficient as a function of the temperature in the range 30–175 °C. Singh et al.[7] have demonstrated the existence of appreciable photoeffects at the semiconductor anode of the n-GaAs|Cp_2Fe^+/Cp_2Fe; $AlCl_3$–BPC| vitreous C cell. Our interest in the electrochemistry of metallocenes in these molten salts has arisen from an assessment of redox systems for photovoltaic devices, in particular because it appears that uncommon oxidation states of certain metallocenes may be stable in these strong Lewis acid, aprotic solvents.[8]

Results and Discussion

Electrochemical Investigations. Cyclic voltammograms illustrated in Figure 1A show that nickelocene (Cp_2Ni) dissolved in a 1:1 molar ratio $AlCl_3$–BPC melt at 40 °C undergoes a reversible 1-electron charge-transfer reaction to the nickelocenium cation (Cp_2Ni^+) at $E_{1/2} \approx$ –0.165 V vs. Al (2:1) reference. The potential shift from the value for the Cp_2Fe/Cp_2Fe^+ couple of approximately –400 mV is consistent with the difference between the two corresponding polarographic waves in 90% ethanolic $HClO_4$ solutions at mercury electrodes.[2a,c] Calculated values for the diffusion coefficient were scattered, probably because of electrode roughness variations ($D = 2.5 \times 10^{-7}$ cm^2 s^{-1} from cyclic voltammetry (Nicholson–Shain constants); $D = 2.9 \times 10^{-7}$ cm^2 s^{-1} from chronoamperometry (40 °C)).

When the red-brown solution of Cp_2Ni in a 1:1 molar ratio melt was adjusted to the 0.95:1 $AlCl_3$:BPC ratio the cyclic voltammograms at low sweep rates (<50 mV s^{-1}) could be interpreted by invoking a slow chemical reaction following charge transfer (Figure 1). The value for the forward anodic oxidation current was unaffected during the course of this experiment (vide infra). Assuming a simple EC mechanism, we estimated the mean reaction rate of the chemical step from theoretical response curves of the i_p^c/i_p^a ratio[9] to be k_f = 0.030 ± 0.005. This reaction was too slow to be measured conveniently by the double-pulse chronoamperometric technique, and the nature of the follow-up process has not been investigated further by us. Addition of butylpyridinium chloride, to adjust the melt to 0.8:1 molar ratio, caused the formation of a green solution and chemical modification to a Cp_2Ni species which exhibited an irreversible oxidation wave at ~+0.16 V (Figure 2). Readjusting the melt composition to

* To whom correspondence should be addressed at Shell Development Co., Houston, TX 77001.

(1) (a) Department of Electrical Engineering. (b) Department of Chemistry.
(2) See, for example: (a) Page, J. A.; Wilkinson, G. *J. Am. Chem. Soc.* **1952**, *74*, 6149. (b) Cotton, F. A.; Whipple, R. O.; Wilkinson, G. *Ibid.* **1953**, *75*, 3586. (c) Wilkinson, G.; Pauson, P. L.; Cotton, F. A. *Ibid.* **1954**, *76*, 1970. (d) Wilkinson, G.; Birmingham, J. M. *Ibid.* **1954**, *76*, 4281. (e) Tirouflet, J.; Laviron, E.; Dabard, R.; Komenda, J. *Bull. Soc. Chim. Fr.* **1963**, 857.
(3) See, for example: (a) Bublitz, D. E.; Hoh, G.; Kuwana, T. *Chem. Ind. (London)* **1959**, 635. (b) Kuwana, T.; Bublitz, D. E.; Hoh, G. *J. Am. Chem. Soc.* **1960**, *82*, 5811. (c) Biegler, T.; Parsons, R. *J. Electroanal. Chem.* **1970**, *27*, 314. (d) Gubin, S. P.; Smirnova, S. A.; Denisovitch, L. I.; Lubovich, A. A. *J. Organomet. Chem.* **1971**, *30*, 243. (e) Holloway, J. D. L.; Bowden, W. L.; Geiger, W. E., Jr. *J. Am. Chem. Soc.* **1977**, *99*, 7089.
(4) Li Chum, H.; Koch, V. R.; Miller, L. L; Osteryoung, R. A. *J. Am. Chem. Soc.* **1975**, *97*, 3264.
(5) Li Chum, H.; Koran, D.; Osteryoung, R. A. *J. Organomet. Chem.* **1977**, *140*, 349.
(6) Robinson, J.; Osteryoung, R. A. *J. Am. Chem. Soc.* **1979**, *101*, 323.
(7) Singh, P.; Rajeshwar, K.; DuBow, J.; Job, R. *J. Am. Chem. Soc.* **1980**, *102*, 4676.
(8) Gale, R. J.; Singh, P.; Job, R. *J. Organomet. Chem.*, in press.
(9) Nicholson, R. S.; Shain, I. *Anal. Chem.* **1964**, *36*, 706.

0020-1669/81/1320-0040$01.00/0